TOR represses stress responses through global regulation of H3K27 trimethylation in plants

Yihan Dong[1, 3, @], Veli V. Uslu[2, 3, @], Alexandre Berr[1], Gaurav Singh[1], Csaba Papdi[1], Victor A Steffens[2], Thierry Heitz[1] and Lyubov Ryabova[1, @]

1. Institute de Biologie Moléculaire des Plantes, Centre National de la Recherche Scientifique, UPR 2357, Université de Strasbourg, Strasbourg, France.
2. AgroScience GmbH, Neustadt an der Weinstraße, 67435, Germany.
3. These authors contributed equally.

[@]Corresponding authors:
yihan.dong@ibmp-cnrs.unistra.fr
velivural.uslu@agroscience.rlp.de
lyuba.ryabova@ibmp-cnrs.unistra.fr

Summary

Combinations of epigenetic modifications H3K4me3 and H3K27me3 implicate bistable feature which alternates between on and off state allowing rapid transcriptional changes upon external stimuli. Target of Rapamycin (TOR) functions as a central sensory hub to link a wide range of external stimuli to gene expression. However, the mechanisms underlying stimulus-specific transcriptional reprogramming by TOR remains elusive. Our *in silico* analysis in Arabidopsis demonstrates that TOR-repressed genes are associated with either bistable or silent chromatin domains. Both domains regulated by TOR signaling pathway are associated with high level of H3K27me3 deposited by CURLY LEAF (CLF) in specific context with LIKE HETEROCHROMATIN PROTEIN1 (LHP1). Chromatin remodeler SWI2/SNF2 ATPase BRAHMA (BRM) activates TOR-repressed genes only at bistable chromatin domains to rapidly induce biotic stress responses. Here we demonstrated both *in silico* and *in vivo* that TOR represses transcriptional stress responses through global maintenance of H3K27me3.

Introduction

The protein kinase TOR is a conserved sensor of nutrient availability and energy status in eukaryotes, known to regulate many fundamental cellular processes, such as translation, autophagy and cell cycle (Saxton and Sabatini, 2017). In animals, since diet and nutrient exert transgenerational effect, correlations between TOR functions and epigenome variations started to be explored (Laribee and Weisman, 2020). Histone acetylation is the most characterized mark regulated by TOR signaling to control rDNA transcription. Recently, mammalian/mechanistic TOR complex 1 (mTORC1) was found to activate its canonical substrate S6K1 which further phosphorylates H2B to influence global histone methylation (Laribee and Weisman, 2020). Unlike in animals, little is known in plants to link TOR function to epigenetic modifications.

As sessile organisms, plants continuously and rapidly adjust their development to a multitude of environmental stresses that often occur suddenly and/or simultaneously. Beyond stress sensing and signal transduction, plant TOR tunes developmental plasticity via its capacity to re-program the transcriptome (Xiong et al., 2013). This global transcriptional reprogramming is partially mediated by the retention of ethylene-insensitive protein 2 (EIN2) in the cytoplasm to allow gene expression involved in DNA replication and cell wall biosynthesis (Fu et al., 2021). However, it still remains obscure how an active TOR can suppress stress response and defense

mechanism at transcriptional level. Among other mechanisms, epigenetic modifications such as DNA methylation and histone modifications have emerged as fundamental mediators in controlling gene expression. For example, methylation of histone H3 on lysine 27 (H3K27) is classically associated with gene repression, whereas methylation on H3K4 usually increases gene expression. Here we are interested in whether epigenetic modification underlies TOR-mediated transcriptional reprogramming.

Multiple combinations of different epigenetic modifications exist at the whole genome level and contribute to the complexity of epigenetic landscapes. By reducing their dimensionality, a detailed bioinformatic integration of epigenomic data defines distinctive chromatin states (CS) in *A. thaliana* (Sequeira-Mendes et al., 2014). These states display specific features that are linked to inactive or active transcription. Two silent states CS-8 and 9 are enriched in H3K9me2 and H3K27me1 and preferentially mark different chromatin regions. Another inactive state CS-5 represents the typical Polycomb-regulated facultative heterochromatin with abundant H3K27me3. Meanwhile, CS-1, 3 and 6 are characterized by high amounts of active marks (*e.g.*, H3K4me3, H3 acetylation, H3K36me3) and typically found at actively transcribed genes. Interestingly, despite their opposite effect on transcription, H3K4me3 and H3K27me3 can co-reside at a number of dynamically regulated genes in both animals and plants. This feature is the hallmark of CS-2, a state preferentially found at the promoter of genes with transcript amounts similar to the ones marked by CS-5. A bistable model of regulation achieved through the delicate balance between H3K4me3 and H3K27me3 was proposed to poise silenced genes marked by CS-2 for rapid activation upon need (Schwartz et al., 2010; Sneppen and Ringrose, 2019). Adding additional layers of complexity, chromatin-binding proteins like H3K27me3 reader LIKE HETEROCHROMATIN PROTEIN 1 (LHP1) or SWI2/SNF2 ATPase BRAHMA (BRM) further subdivide these chromatin domains into distinct subdomains (Gomez-Zambrano et al., 2019; Liu et al., 2018; Torres and Deal, 2019).

In this study, we show that specific epigenetic features represent a dynamic hallmark of stimulus-specific transcriptional responses mediated by TOR signaling upon environmental stimuli. We demonstrate that active TOR represses genes associated with bistable (CS2) or silent chromatin domains (CS5) by mediating the deposition of H3K27me^3 via CLF and LHP1. We propose a model in which environmental stimuli inhibit TOR, which subsequently allows BRM to reduce repression of bistable domains to rapidly activate biotic stress specific gene expression.

Results

TOR-repressed genes are associated with CS-2 and CS-5 at the transcription start site

First, we performed gene ontology (GO) enrichment analysis to assess whether specific functional categories are enriched in any of the previously described chromatin states (Sequeira-Mendes et al., 2014). Arabidopsis genes were individually assigned to one of the nine chromatin states based on the chromatin state present at their TSS. Surprisingly, each of the nine chromatin states were specifically enriched in distinct functional categories (Supplementary table 1). Indeed, genes related to protein and RNA processes appeared highly enriched in CS-1, 3 and 6, which are characterized by the presence of active epigenetic marks. The Polycomb-associated CS-5 contained significantly more transcription, cell differentiation, and redox-regulation related genes. Abiotic and biotic stress genes are overrepresented in the bistable CS-2. Worth noting, functional categories enriched in CS-2 resemble the primary target genes in stress and immune response pathways repressed by TOR (Dong et al., 2015).

To analyze particular chromatin state enrichments among TOR-repressed transcripts, from published datasets we extracted a list of genes up-regulated (fold change>2.0; p<0.05) upon TOR inhibition by AZD8055 (AZDup, 1583 genes) or RNA interference (TOR-RNAi, 369 genes) (Caldana et al., 2013; Dong et al., 2015). 233 genes upregulated in both conditions were significantly enriched at their TSS in the bistable CS-2 and also in the canonical Polycomb CS-5 (fig. 1a). These findings suggest that the repression of gene expression by TOR is achieved through either CS-2 or CS-5, two chromatin states sharing high levels of the repressive modification H3K27me3. Furthermore, by distinguishing up-regulated genes depending on their fold change, we observed that the CS-5 enrichment gradually increases with the fold change, which is also the case for CS-2 but not beyond 16-fold change. In addition, more than half of the CS-2 genes change only 2-4-fold (fig. 1b and supplementary fig. 1). This striking difference could reflect the bistability of CS-2, in which frequent switches between active and silent state may occur, resulting in a low rate of basal transcription and finetuning upon TOR inhibition. TOR-repressed genes marked by the monostable silent CS-5 are likely under complete repression.

Next, using GO analysis, we tested whether AZDup genes marked by either CS-2 or CS-5 are enriched in particular functional categories. Interestingly, AZDup genes marked by CS-2 are enriched in biotic stress and defense mechanisms mediated by phytohormone signaling (fig. 1c, d), whereas, abiotic stress related genes involved in oxidative stress and hypoxia response are more abundant among AZDup genes with CS-5 features (fig. 1e). These findings indicate that the TOR suppressed genes are preset by bistable CS-2 and silent CS-5 properties and specific signals can attenuate TOR-mediate repression towards CS-2 and CS-5 genes.

The chromatin context of TOR-responsive genes coordinately repressed by CLF and LHP1 specify their biological function

Based on the preferential association between TOR repressed genes and CS-2/5, both characterized by the presence of H3K27me3, we hypothesized that a functional link may exist between chromatin factors involved in H3K27me3 deposition and TOR. We tested this hypothesis by collating the TOR repressed gene set with transcript profiles of Polycomb mutants. CURLY LEAF (CLF), a Polycomb group protein (PcG), is known to be a major H3K27 tri-methylase in plants (Mozgova and Hennig, 2015). A total of 84 genes are shared between AZDup and those genes upregulated in the loss-of-function *clf28* and *clf29* mutants (fig. 2a). These shared genes display a significantly higher association with CS-2 (OR=3.86) at their TSS than the AZDup or the up-regulated genes in either *clf28* or *clf29* (fig. 2b and supplementary fig. 2a). Reinforcing this positive association, the CS-2 enrichment of AZDup decreases when the genes up-regulated in *clf* mutants are excluded (AZDno*clf28*/*29*; fig. 2b). Similarly, the CS-5 enrichment is remarkably higher for genes upregulated in both AZDup and *clf* mutants compared to the genes upregulated only in AZDup (AZDno*clf28*/29; fig. 2b and supplementary fig. 2a). These observations suggest a synergistic enrichment of CLF and TOR repressed genes in CS-2 and CS-5, two chromatin states characterized by a high level of the repressive modification H3K27me3. Furthermore, the GO analysis of the 84 commonly up-regulated genes between AZDup and *clf* mutants points toward a chromatin state dependent functional categorization. Indeed, commonly up-regulated genes within CS-2 are significantly enriched in GO categories related to biotic and abiotic stress responses, while the ones within CS-5 are specifically enriched in the GO term related to redox processes (fig. 2c).

PcGs are generally classified into two major complexes named Polycomb Repressive Complexes (PRC1 and PRC2) and CLF, a major PCR2 subunit, selectively collaborates with different PcGs partners to achieve gene repression in distinct developmental programs. Among these partners, LHP1, as a CLF cofactor, was previously demonstrated to contribute to this selectivity with genes up-regulated in different PcG mutants being separated in two distinct main groups based on their dependency on LHP1 repression (Wang et al., 2016). A first group represents genes commonly up-regulated in *clf* and *lhp1* mutants and may correspond to direct targets of CLF and LHP1 (*i.e.,* here after named CLF-LHP1-dependent genes). The second one refers to genes more specifically affected in PRC1 mutants such as the double mutant for the catalytic factors AtRING1A and AtRING1B (*i.e.,* here after named PRC1-PRC2 dependent genes). Thus, to dissect the relationship between TOR and CLF transcriptional repression and explore its dependency toward LHP1, we tested overlaps between these two groups and AZDup genes. A significant overlap was observed between AZDup and CLF-LHP1-dependent genes (fig. 2d), while it was not the case with PRC1-PRC2 dependent genes (fig. 2d). This result suggests that CLF and LHP1 may work concertedly to participate in the repression of TOR specific target genes.

We further investigated the link between TOR and LHP1 by focusing on the 111 genes commonly upregulated by AZD8055 and in the *lhp1* mutant (fig. 2e). In a manner similar to genes co-upregulated by AZD and *in clf mutants*, these genes showed a significant enrichment in both CS-2 and CS-5 (fig. 2f and supplementary fig. 2b). When we analyzed overlap between LHP1-target genes and genes up-regulated by AZD8055, we found that 445 out of 1583 AZDup genes are indeed targeted by LHP1 (fig. 2g). Interestingly, the CS-2 enrichment of AZDup genes was decreased when LHP1 targets were excluded, whereas genes both upregulated by AZD and targeted by LHP1 present an increased CS-2 enrichment compared to genes *sole* upregulated by AZD or targeted by LHP1 (fig. 2h). In addition, we noted that the LHP1 targeting also increase the CS-5 enrichment of AZDup genes (fig. 2h). This observation is reinforced by the fact that when LHP1 direct targets were excluded the association between AZDup and CS-5 dropped dramatically (fig.2h and supplementary fig. 2c). Finally, we investigated whether LHP1 targeting specifies TOR functions using GO analysis. Interestingly, the functional annotation obtained with the CS-2 subset of AZDup genes targeted by LHP1 is mainly linked to biotic and abiotic stress-related functions (fig. 2i). On the other hand, the functional annotations obtained with the CS-5 subset of AZDup genes targeted by LHP1 appears mainly related to oxidative stress and hypoxia responses (fig 2j). Together, our results indicate that besides being regulated jointly by CLF and LHP1, TOR repressed targets may further split in distinct functional categories depending on their respective CS-2 or CS-5 chromatin context.

BRM is important for activating genes associated with CS-2, when TOR is down-regulated in response to biotic stress

TrxG proteins are evolutionarily conserved chromatin-modifying factors that antagonize PcG repression and interactions between PcG/TrxG support a molecular basis for chromatin bistability (Ringrose, 2017; Sneppen and Ringrose, 2019). Among TrxG proteins, the SWItch/Sucrose Non-Fermentable (SWI/SNF)-type protein BRAHMA (BRM) was find to restrict CLF occupancy/activity at many developmental genes (Shu et al., 2020). We therefore wondered whether the TrxG protein BRM would participate in establishing bistable chromatin at the CS-2 subset of TOR regulated genes. Considering BRM as an activator of gene expression, we observed a significant overlap between AZDup genes and genes down-regulated in *brm1* mutant (supplementary fig. 3a) and also found that 57% of AZDup genes are BRM targets (fig.

3a). Moreover, the CS-2 enrichment among BRM targets was further reinforced when including the overlap with AZDup (fig. 3b). This is especially true when compared to the CS-2 enrichment of AZDup genes not targeted by BRM or BRM targets not among AZDup (fig. 3b and supplementary fig. 3b). Then, our GO analysis demonstrates that AZDup genes which overlap with BRM target genes are mostly biotic stress related, while BRM targets not suppressed by TOR are mostly related to transcriptional regulation (fig. 3c).

While keeping in mind the bistability of CS-2, we analyzed the overlap between the TrxG component BRM targets and the PcG component LHP1 targets. A total of 1216 genes are co-targeted by BRM and LHP1, among which 240 genes appeared as AZDup (supplementary fig. 3c). Further reinforcing a functional link between TOR repressed genes and bistable chromatin, these genes show the highest CS-2 enrichment in this study. Furthermore, this result suggests that BRM and LHP1 together act on TOR repressed genes to establish chromatin bistability (supplementary fig. 3d). Our GO analysis reveals a preferential enrichment in biotic stress related terms for the CS-2 category, while the Cs-5 was preferentially enriched in GO terms related to oxidative stress and hypoxia. This observation suggests a functional dichotomy between AZDup genes co-targeted by BRM and LHP1 in CS-2 and AZDup genes targeted by LHP1 in CS-5. Notably, the 976 genes co-targeted by BRM and LHP1 but not upregulated upon TOR inhibition preferentially belong to TOR-independent functional categories, *e.g.*, salinity response, auxin and gibberellin signaling at CS2; transcription regulation and cell wall modification at CS-5 (supplementary fig. 3e-g).

The proposed functional dichotomy among TOR repressed genes implies that, within CS-2, BRM may specifically activate genes involved in defense mechanism upon TOR inhibition by a biotic stress signal. In agreement, it has been previously shown that over-expression of TOR increased the susceptibility to both bacterial and fungal infections (De Vleesschauwer et al., 2018). To explore in more details the role of BRM in regulating biotic stress related genes within CS-2, *brm5* mutants were inoculated with the fungal pathogen *Botrytis cinerea.* Compared to the wild-type control (Col-0), *brm5* mutants exhibited an enhanced susceptibility to *B. cinerea* with a significant increase in lesion size while *clf29* did not (fig. 3d, e). Supporting our *in-silico* analyses, opposite sensitivities were observed when mutants were tested for their response to hypoxia caused by submergence. Indeed, while *brm5* behaved similarly as Col0, *clf29* mutants were significantly less resistant to submergence (fig. 3f, g). Together, our results indicate that BRM contributes to the functional specification of TOR responding genes.

TOR coordinates global H3K27me3 level at different growth and developmental stages

The different correlations highlight a functional link between TOR and H3K27me3 transcriptional repression. We therefore hypothesize that the activation of TOR repressed targets associated with CS-2 and CS-5 may require an active removal of H3K27me3. To test this hypothesis, Arabidopsis were treated for 24 hours with AZD8055 to inhibit TOR. Interestingly, AZD8055 treatment provoked a decrease in the global level of H3K27me3 (fig.4a). In a complementary approach, we also explore the impact of a TOR inhibition on the global level of H3K27me3 by means of quantitative immuno-staining on root nuclei. In agreement with the pharmaceutical inhibition of TOR by AZD8055, the level of fluorescence intensity of H3K27me3 was significantly decreased upon inhibition of TOR by estradiol-inducible TOR RNAi with fluorescence levels were intermediate between those of the mock-treated control and the *clf29* mutant (fig. 4b). Then we challenged a *clf29* with TOR inhibition.

clf29 mutant did not respond to AZD8055 treatment (fig. 4c), which suggested that growth arrest by TOR inactivation was largely dependent on loss of H3K27me3.

Both TOR kinase and H3K27me3 are important for photomorphogenesis (Charron et al., 2009; Pfeiffer et al., 2016). Charron et al., 2019 showed a global increase of H3K27me3 level across chromosomes in the seedlings transferred from darkness to light. In the darkness, COP1 represses TOR activity to allow skotomorphogenesis (fig. 4d). To gain more biological insight, we further tested whether H3K27me3 level is correlated with TOR activity during photomorphogenesis. In agreement with published CHIP-seq data, light-grown seedling had higher H3K27me3 than etiolated seedlings in the dark. AZD8055 treatment significantly reduced the H3K27me3 level. In the *cop1* mutant where TOR is pre-induced in the dark (Pfeiffer et al., 2016), H3K27me3 level was also maintained high to allow photomorphogenesis of *cop1* in the dark (fig. 4e). We conclude that TOR can recruit histone-modifying complexes such as CLF/ LHP1 to regulate transcriptome via H3K27 tri-methylation.

Discussion

Our findings presented here, strongly suggest a model in which TOR amplifies the CLF function associated with LHP1 to increase the level of H3K27 tri-methylation mainly through the CLF-LHP1 in state 2 genes enriched in biotic stress responses and CS-5 genes involved in redox processes and hypoxia responses. Moreover, in conditions of TOR inactivation, BRM is responsible for removal of inhibitory H3K27 tri-methylation, possibly via demethylase REF6 (Li et al., 2016), to activate CS-2 genes mainly involved in biotic stress responses (fig. 4f). We present how a certain stress signal can go through the central master regulator TOR and target specific genomic loci. Facing the environmental challenges, plants inactivate TOR as a common response to save energy and induce stress responsive genes. When TOR is inactivated, BRM is required to induce a subset of genes involved in biotic stress.

H3K27me3 has been extensively studied in eukaryotes. This conserved histone modification targets key developmental genes but shows a drastically different landscape in plants and animals. PRC2 complex can read and write H3K27me3 and is associated with DNA in a long-range, which results in large patches of H3K27me3, in animals. In plants, H3K27me3 marks more often a single gene (Mozgova and Hennig, 2015). This difference might contribute to the dynamic regulation of gene expression by H3K27me3 in plants. Comparing to animals, plants are sessile and must constantly alter the developmental program facing environmental stimuli. High H3K27me3 level is tightly associated with cell stemness and represses early differentiation genes. In plants, TOR is highly expressed in the meristematic tissues, indicating high H3K27me3 level according to this work. Here discovered TOR-H3K27me3 relay may contribute significantly to the meristem function and plant regeneration ability which represents a fundamental difference to animals.

LHP1, a plant-specific polycomb protein, works in collaboration with CLF to deposit and spread H3K27me3, which distinguishes CLF function from PRC1-PRC2 complex (Wang et al., 2016). Strikingly, CLF and LHP1 targets are exclusively enriched in CS-5, whereas up-regulated genes in loss-of-function mutants are enriched in both CS-2 and CS-5 (fig. 2 and supplementary fig. 4a). This further supports that H3K4me3 and H3K27me3 marking CS-2 are bistable instead of bivalent, which may explain the loss of targets identification by CHIP. Moreover, AZDup genes targeted by CLF is also underrepresented (supplementary fig. 4b). CLF-LHP1 mediates largely expression of TOR-responsive genes involved in biotic stress response and redox process.

Indeed, biotic stress response genes are marked by bistable chromatin features (CS-2), which likely indicates a rapid responsive state to the environmental stimuli. In comparison, CS-5 is stably repressed which is more associated with house-keeping function (supplementary table 1).

BRM is a phosphorylation target of the ABA-SnRK2 relay, which reciprocally regulated the TOR signaling pathway (Peirats-Llobet et al., 2016; Wang et al., 2018). TOR could inhibit BRM function through silencing ABA signaling. Moreover, BRM protein sequence contains several TOR phosphorylation consensus sites, suggesting that specific phosphorylation of BRM by TOR and/or SnRK2 can regulate its function (Van Leene et al., 2019). Many studies showed the nuclear localization of SnRK2 kinase (Peirats-Llobet et al., 2016). The canonical TOR substrate S6K2 localizes in the nucleus and phosphorylates BIN2 functioning in brassinosteroid pathway (Mahfouz et al., 2006; Xiong et al., 2017).

In the cytoplasm, TOR might regulate H3K27me^3 through mRNA translation of several key enzymes involved in H3K27 methylation or demethylation. La-related protein 1 (LARP1) is a RNA binding protein conserved across eukaryotes regulating 5' terminal oligopyrimidine motif (5'TOP) mRNA translation. Recent studies showed that TOR phosphorylates LARP1 in plants and can regulate the translation efficiency of 5'TOP-mRNAs that encode proteins involved in chromatin remodeling, e.g. LHP1 (Scarpin et al., 2020; Van Leene et al., 2019). In addition, TOR may regulate the availability of a methylation substrate, S-adenosyl-methionine (SAM) that functions in the methionine-folate cycle. Interestingly, MTHFD1 is a folate cycle enzyme impacting global DNA methylation in plants through SAM availability (Groth et al., 2016). In animals, mTORC1 senses SAM levels through SAMTOR and MTHFD transcription under tight control of mTORC1 (Ben-Sahra et al., 2016; Gu et al., 2017). However, it remains unknown whether plant TOR modulates DNA or histone methylation through SAM metabolism in plants. SAMTOR seems to be also a metazoan invention.

Since H3K27me^3 occupies the intergenic regions, we speculate that TOR impacts transcriptome through intergenic non-coding RNAs. In plants, AZD8055-mediated TOR inhibition can induce long non-coding RNA expression which is often marked by H3K27me^3 (Song et al., 2018). This suggests that global decrease of H3K27me^3 level in conditions of TOR inactivation could also affect transcription or translation through long non-coding RNAs. Our finding reveals a missing link from environmental sensing to epigenetic regulation. In the future, it will be of great interest to dissect this signaling pathway and investigate mechanism of the TOR-dependent epigenetic reprogramming at different stages of developmental transition and responses to environment.

Acknowledgement

We thank D. Janocha (University of Heidelberg) for providing *cop1* mutants, French Agence Nationale de la Recherche— ANR-18-CE13-0019 – ReinitiaTOR to L.R. and 2020 Marie Curie fellowship 885864 TORinacTIon MSCA-IF-EF-ST to Y.D.

Author contribution

Y.D. and V.U.U. initiated the project. Y.D., V.U.U., A.B. and C.P. contributed to experiment design and project development. Y.D. coordinated the project and performed experiments. V.U.U. and V.A.S performed bioinformatic analysis. A.B. and G.S. performed immuno-staining.

Y.D. and T.H. performed *B. cinerea* infection. Y.D., V.U.U. and A.B. made figures and wrote the manuscript. C.P., T.H. and L.R. revised the manuscript.

Declaration of interest

The authors declare that the research was conducted in the absence of any commercial or financial relationships that could result in any potential conflict of interest.

Methods

Plant materials and growth condition

Arabidopsis thaliana mutant plants, as well as wild-type control plants were the Columbia (Col-0) ecotype. Wild-type plants (N1092) and *brm-5* (N68980) were gained from the European Arabidopsis Stock Centre. *clf-29* (SALK_021003) mutant was described in Wang et al., 2016 (Wang et al., 2016). *cop1-4* was described in (Pfeiffer et al., 2016). ß-estradiol inducible TOR-RNAi line was described in (Xiong et al., 2013). All seedlings were grown on 1/2MS medium (pH5.7, 0.8% agar) in a long-day climate chamber (16 h light/8 h dark; 80-100 µmol m-2s-1; 22°C day/18°C night; 50% humidity). Chemical inhibitor treatments were performed with media containing 0.2 µM AZD-8055 for 10 days or 1 µM for 24 hours. Submergence was performed with 5 week soil-grown plants for 24 hours and recovered for 1 week in the short-day climate chamber (12 h light/12 h dark).

Western blot

For immunological detection, total soluble proteins were extracted from 50 mg plant materials with 250 µl 2x Laemmli buffer. Proteins were denatured for 5 min at 95°C and separated on 15% SDS-PAGE. Subsequently, proteins were blotted to PVDF membrane. The primary antibodies anti-H3K27me3 (1:5000, Agrisera, AS16-3193) and anti-H3 (1:5000, Agrisera, AS10-710) were detected using the HRP-conjugated secondary antibody (1:20,000).

Fungi infection

B. cinerea was inoculated on 5-week-old soil-grown plants in a short-day chamber (12 h light/12 h dark; 80-100 µmol m-2s-1; 22°C day/18°C night; 50% humidity). For the lesion assay, 5-µL droplets of *B. cinerea* spore suspension were placed directly on the upper surface of the leaf. After inoculation, plants were kept with full humidity to facilitate the infection. Lesions were measured 3 days after the inoculation.

Chromatin state enrichment analysis

Chromatin states were defined based on Hidden Markov Model (HMM) and previously defined coordinates were extracted (Sequeira-Mendez et al., 2014). The gene sets are given in supplementary table 2. Transcription start sites (TSS) and transcription termination sites (TTS) are downloaded from www.arabidopsis.org (TAIR10). An array is formed for each region of interest. GenomicRanges R-package was used to match the genes in each set with a chromatin state (Lawrence et al., 2013). The enrichment of chromatin states were calculated by odd ratio (OR) and False Discovery Rate (FDR) adjusted p values were used to define the significance of OR. Statistical comparison of different ORs were performed by Fisher's exact test and statistical significance threshold is taken as $p<0.05$.

Immunostaining and microscopy

Immunostaining was performed as described previously (Batzenschlager et al., 2015) on 7-days-old *in-vitro* grown seedlings of Col-0, TOR-RNAi and *clf-29* treated or not for 24h with 10

µM ß-estradiol. Antibodies used for immunostaining were the anti-H3K27me3 (1:500) and the Alexa fluor-488 dyes-conjugated secondary antibody (1:1000, Life Technologies, A-11008). The H3K27me3 signal intensity for each nucleus was calculated relative to the intensity of DAPI using ImageJ software. Confocal images were acquired with a Zeiss LSM-700 microscope with a 63x/1.01 objective.

References

Batzenschlager, M., Lermontova, I., Schubert, V., Fuchs, J., Berr, A., Koini, M.A., Houlne, G., Herzog, E., Rutten, T., Alioua, A., *et al.* (2015). Arabidopsis MZT1 homologs GIP1 and GIP2 are essential for centromere architecture. Proc. Natl. Acad. Sci. U. S. A. *112*, 8656-8660.

Ben-Sahra, I., Hoxhaj, G., Ricoult, S.J.H., Asara, J.M., and Manning, B.D. (2016). mTORC1 induces purine synthesis through control of the mitochondrial tetrahydrofolate cycle. Science *351*, 728-733.

Caldana, C., Li, Y., Leisse, A., Zhang, Y., Bartholomaeus, L., Fernie, A.R., Willmitzer, L., and Giavalisco, P. (2013). Systemic analysis of inducible target of rapamycin mutants reveal a general metabolic switch controlling growth in *Arabidopsis thaliana*. The Plant Journal *73*, 897-909.

Charron, J.B., He, H., Elling, A.A., and Deng, X.W. (2009). Dynamic landscapes of four histone modifications during deetiolation in Arabidopsis. Plant Cell *21*, 3732-3748.

De Vleesschauwer, D., Filipe, O., Hoffman, G., Seifi, H.S., Haeck, A., Canlas, P., Van Bockhaven, J., De Waele, E., Demeestere, K., Ronald, P., *et al.* (2018). Target of rapamycin signaling orchestrates growth-defense trade-offs in plants. New. Phytol. *217*, 305-319.

Dong, P., Xiong, F., Que, Y., Wang, K., Yu, L., Li, Z., and Maozhi, R. (2015). Expression profiling and functional analysis reveals that TOR is a key player in regulating photosynthesis and phytohormone signaling pathways in Arabidopsis. Frontiers in Plant Science *6*.

Fu, L., Liu, Y., Qin, G., Wu, P., Zi, H., Xu, Z., Zhao, X., Wang, Y., Li, Y., Yang, S., *et al.* (2021). The TOR-EIN2 axis mediates nuclear signalling to modulate plant growth. Nature. *591*, 288-292.

Gomez-Zambrano, A., Merini, W., and Calonje, M. (2019). The repressive role of Arabidopsis H2A.Z in transcriptional regulation depends on AtBMI1 activity. Nat. Commun. *10*, 2828.

Groth, M., Moissiard, G., Wirtz, M., Wang, H.F., Garcia-Salinas, C., Ramos-Parra, P.A., Bischof, S., Feng, S.H., Cokus, S.J., John, A., *et al.* (2016). MTHFD1 controls DNA methylation in Arabidopsis. Nat. Commun. *7*.

Gu, X., Orozco, J.M., Saxton, R.A., Condon, K.J., Liu, G.Y., Krawczyk, P.A., Scaria, S.M., Harper, J.W., Gygi, S.P., and Sabatini, D.M. (2017). SAMTOR is an S-adenosylmethionine sensor for the mTORC1 pathway. Science *358*, 813-818.

Laribee, R.N., and Weisman, R. (2020). Nuclear Functions of TOR: Impact on Transcription and the Epigenome. Genes (Basel) *11*.

Lawrence, M., Huber, W., Pages, H., Aboyoun, P., Carlson, M., Gentleman, R., Morgan, M.T., and Carey, V.J. (2013). Software for computing and annotating genomic ranges. PLoS Comput. Biol. *9*, e1003118.

Li, C., Gu, L., Gao, L., Chen, C., Wei, C.Q., Qiu, Q., Chien, C.W., Wang, S., Jiang, L., Ai, L.F., *et al.* (2016). Concerted genomic targeting of H3K27 demethylase REF6 and chromatin-remodeling ATPase BRM in Arabidopsis. Nat. Genet. *48*, 687-693.

Liu, Y., Tian, T., Zhang, K., You, Q., Yan, H., Zhao, N., Yi, X., Xu, W., and Su, Z. (2018). PCSD: a plant chromatin state database. Nucleic Acids. Res. *46*, D1157-D1167.

Mahfouz, M.M., Kim, S., Delauney, A.J., and Verma, D.P. (2006). Arabidopsis TARGET OF RAPAMYCIN interacts with RAPTOR, which regulates the activity of S6 kinase in response to osmotic stress signals. Plant Cell *18*, 477-490.

Mozgova, I., and Hennig, L. (2015). The polycomb group protein regulatory network. Annu. Rev. Plant Biol. *66*, 269-296.

Peirats-Llobet, M., Han, S.K., Gonzalez-Guzman, M., Jeong, C.W., Rodriguez, L., Belda-Palazon, B., Wagner, D., and Rodriguez, P.L. (2016). A Direct Link between Abscisic Acid Sensing and the Chromatin-Remodeling ATPase BRAHMA via Core ABA Signaling Pathway Components. Mol. Plant *9*, 136-147.

Pfeiffer, A., Janocha, D., Dong, Y., Medzihradszky, A., Schöne, S., Daum, G., Suzaki, T., Forner, J., Langenecker, T., Rempel, E.*, et al.* (2016). Integration of light and metabolic signals for stem cell activation at the shoot apical meristem. eLife *5*, e17023.

Ringrose, L. (2017). Noncoding RNAs in Polycomb and Trithorax regulation: a quantitative perspective. Annu. Rev. Genet. *51*, 385-411.

Saxton, R.A., and Sabatini, D.M. (2017). mTOR Signaling in Growth, Metabolism, and Disease. Cell *169*, 361-371.

Scarpin, M.R., Leiboff, S., and Brunkard, J.O. (2020). Parallel global profiling of plant TOR dynamics reveals a conserved role for LARP1 in protein translation. Elife 9, e58795.

Schwartz, Y.B., Kahn, T.G., Stenberg, P., Ohno, K., Bourgon, R., and Pirrotta, V. (2010). Alternative epigenetic chromatin states of polycomb target genes. PLoS Genet. *6*, e1000805.

Sequeira-Mendes, J., Araguez, I., Peiro, R., Mendez-Giraldez, R., Zhang, X., Jacobsen, S.E., Bastolla, U., and Gutierrez, C. (2014). The functional topography of the Arabidopsis genome is organized in a reduced number of linear motifs of chromatin states. Plant Cell *26*, 2351-2366.

Shu, J., Chen, C., Li, C., and Cui, Y. (2020). The complexity of PRC2 catalysts CLF and SWN in plants. Biochem. Soc. Trans. *48*, 2779-2789.

Sneppen, K., and Ringrose, L. (2019). Theoretical analysis of Polycomb-Trithorax systems predicts that poised chromatin is bistable and not bivalent. Nat. Commun. *10*, 2133.

Song, Y., Li, L., Yang, Z., Zhao, G., Zhang, X., Wang, L., Zheng, L., Zhuo, F., Yin, H., Ge, X.*, et al.* (2018). Target of Rapamycin (TOR) regulates the rxpression of lncRNAs in response to abiotic stresses in cotton. Front. Genet. *9*, 690.

Torres, E.S., and Deal, R.B. (2019). The histone variant H2A.Z and chromatin remodeler BRAHMA act coordinately and antagonistically to regulate transcription and nucleosome dynamics in Arabidopsis. Plant J. *99*, 144-162.

Van Leene, J., Han, C., Gadeyne, A., Eeckhout, D., Matthijs, C., Cannoot, B., De Winne, N., Persiau, G., Van De Slijke, E., Van de Cotte, B.*, et al.* (2019). Capturing the phosphorylation and protein interaction landscape of the plant TOR kinase. Nat. Plants *5*, 316-327.

Wang, H., Liu, C., Cheng, J., Liu, J., Zhang, L., He, C., Shen, W.H., Jin, H., Xu, L., and Zhang, Y. (2016). Arabidopsis flower and embryo developmental genes are repressed in seedlings by different combinations of Polycomb group proteins in association with distinct sets of cis-regulatory elements. PLoS Genet. *12*, e1005771.

Wang, P., Zhao, Y., Li, Z., Hsu, C.C., Liu, X., Fu, L., Hou, Y.J., Du, Y., Xie, S., Zhang, C.*, et al.* (2018). Reciprocal regulation of the TOR kinase and ABA receptor balances plant growth and stress response. Mol. Cell *69*, 100-112 e106.

Xiong, F., Zhang, R., Meng, Z., Deng, K., Que, Y., Zhuo, F., Feng, L., Guo, S., Datla, R., and Ren, M. (2017). Brassinosteriod Insensitive 2 (BIN2) acts as a downstream effector of the Target of Rapamycin (TOR) signaling pathway to regulate photoautotrophic growth in Arabidopsis. New Phytol. *213*, 233-249.

Xiong, Y., McCormack, M., Li, L., Hall, Q., Xiang, C., and Sheen, J. (2013). Glucose-TOR signalling reprograms the transcriptome and activates meristems. Nature *496*, 181-186.

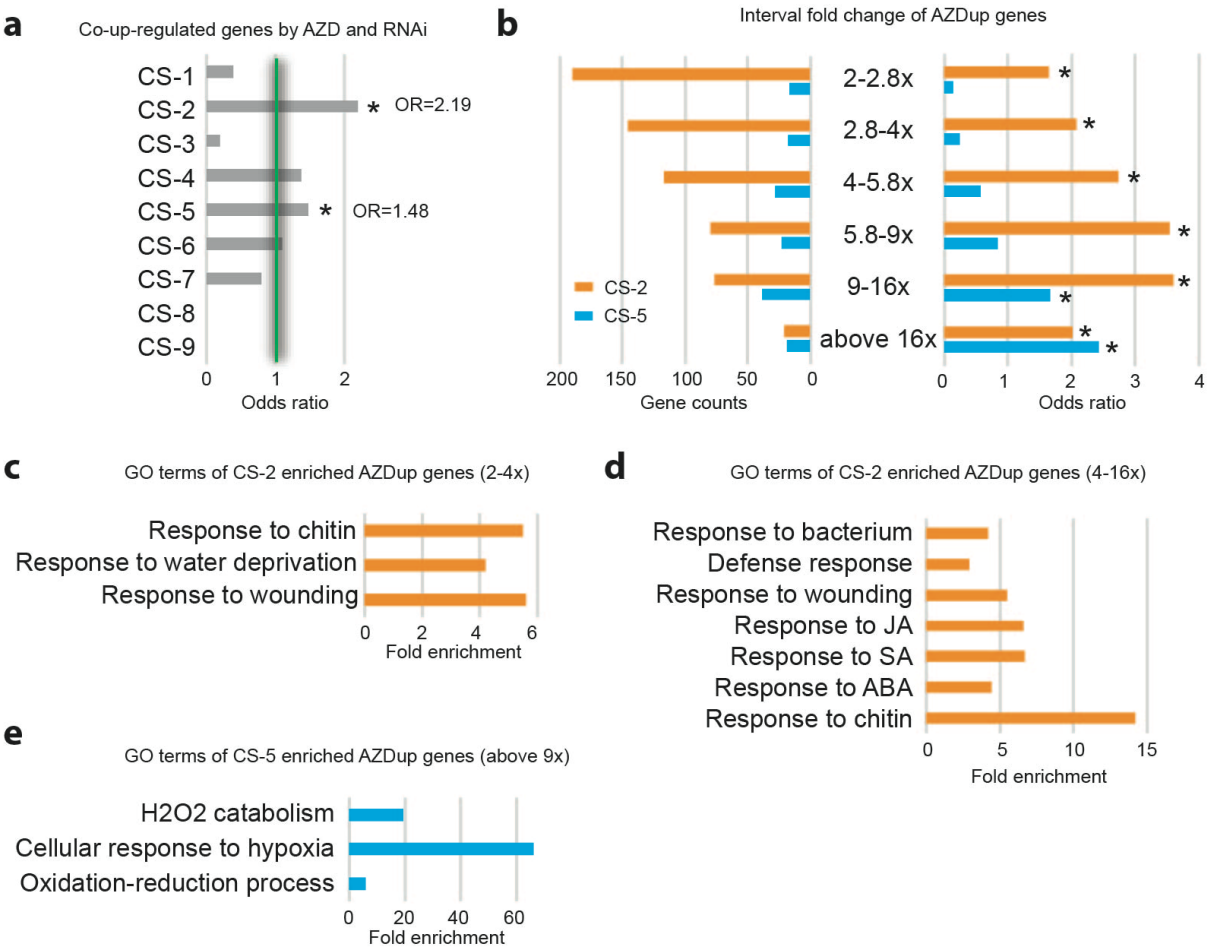

Figure 1 CS-2 and -5 specify the functional groups of TOR-responsive genes. (a) Enrichment of co-up-regulated genes by both AZD8055 and TOR RNAi in different chromatin states (CS; *, odds ratio>1 and p<0.05). Different chromatin states were defined by Sequeira-Mendes *et al*., 2014 (Sequeira-Mendes et al., 2014). (b) Enrichment and gene counts of different interval fold-change of up-regulated genes by AZD8055 (AZDup) in CS-2 and CS-5 (*, odds ratio>1 and p<0.05). (c-e) Functional category analysis of AZDup CS-2 genes with 2-4 fold, 4-16 fold and CS-5 genes up-regulated at least 9 fold (p<0.01, FDR<0.1).

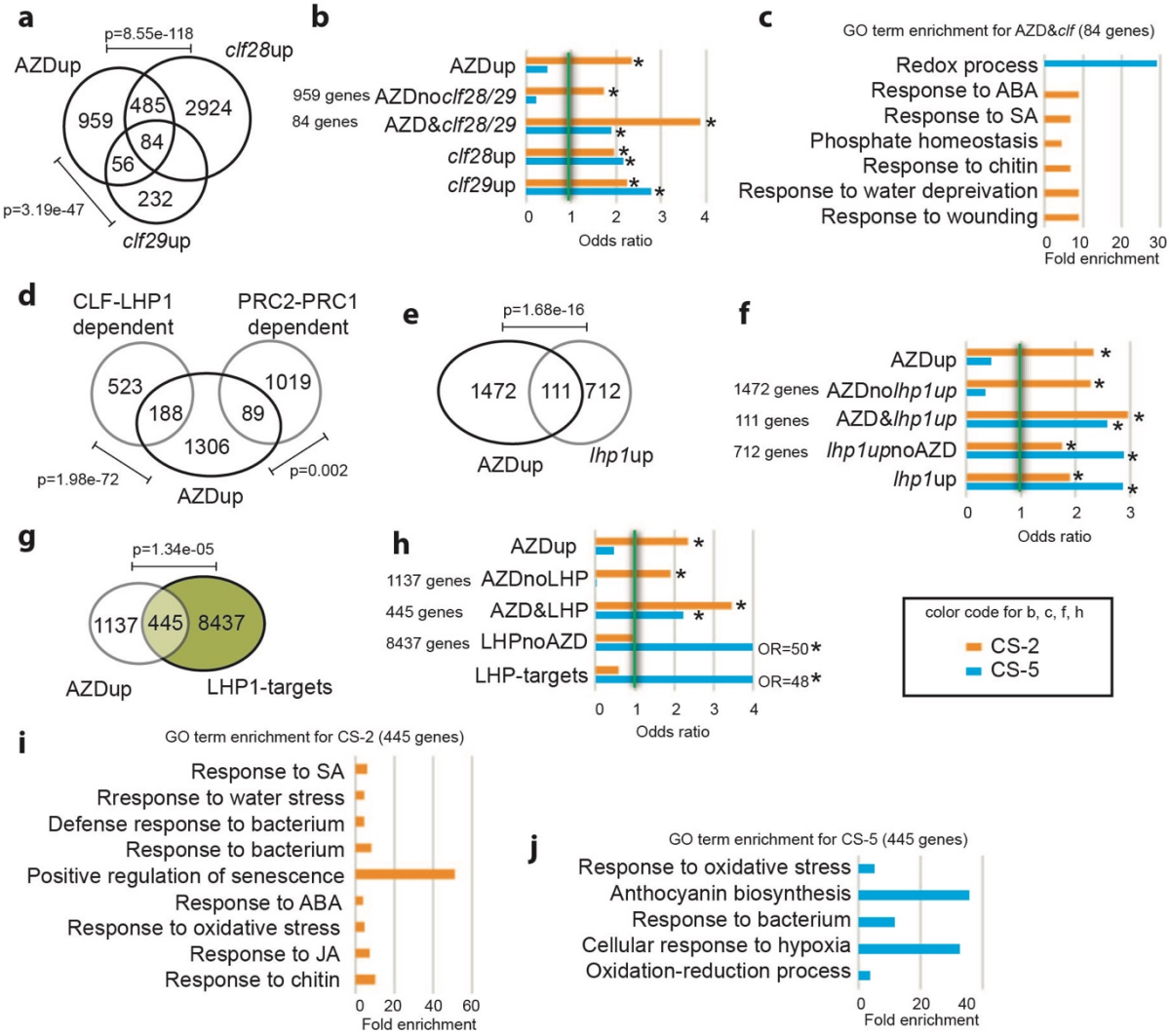

Figure 2 TOR represses both CS-2 and 5 genes via CLF in specific context with LHP1. (a) overlap of up-regulated genes by AZD8055 (AZDup), in *clf28* mutant (*clf28*up, hypergeometric test) and in *clf29* mutant (*clf29*up2x, hypergeometric test). (b) Enrichment of genes from different intersection between AZDup, *clf28*up and *clf29*up presented in (a) (*, OR>1 and p<0.05). (c) Functional category analysis of co-up-regulated genes by AZD8055 and in *clf28/29* enriched in CS-2 and CS-5 (p<0.01, FDR<0.1). (d) overlap of up-regulated genes by AZD8055 (AZDup) and context-dependent CLF regulated genes (hypergeometric test). (e) overlap of up-regulated genes by AZD8055 (AZDup) and in lhp1 mutant (*lhp1*up) (hypergeometric test). (f) Enrichment of genes from different intersection between AZDup and *lhp1*up presented in (e) (*, OR>1 and p<0.05). (g) overlap between genes up-regulated by AZD8055 (AZDup) and LHP1 target genes (hypergeometric test). (h) Enrichment of genes from different intersection between AZDup2x and LHP1 targets presented in (g) (*, OR>1 and p<0.05). (i, j) Functional category analysis of LHP1-targeted AZDup genes from CS-2 (i) and CS-5 (j) (p<0.01, FDR<0.1).

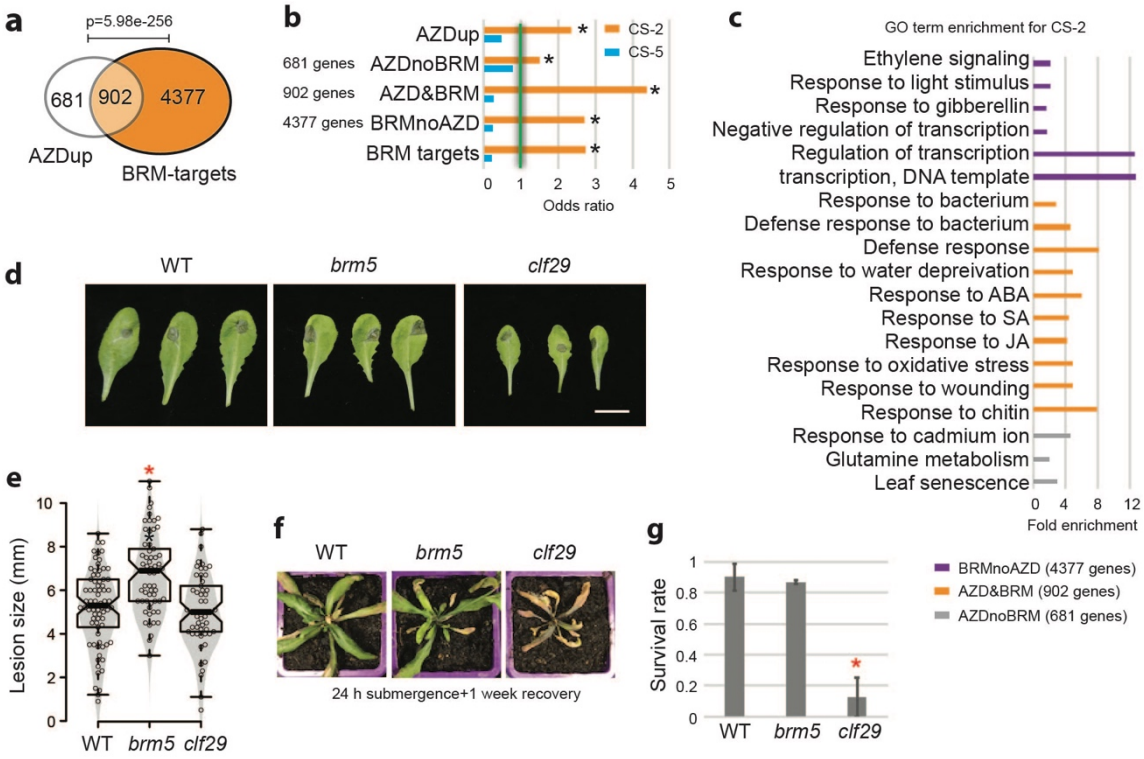

Figure 3 BRM specifically activates CS-2 genes to induce biotic stress response upon TOR inhibition. (a) overlap of up-regulated genes by AZD8055 (AZDup) and BRM target genes (hypergeometric test). (b) Enrichment of genes from different intersection between AZDup and BRM targets presented in (a) (*, OR>1 and p<0.05). (c) Functional category analysis of CS-2 enriched AZDup genes and BRM targets presented in (b) (p<0.01, FDR<0.1). (d) leaf phenotype and (e) lesion size of *brm5* and *clf29* mutants infected by *B. cinerea* compared to col-0 (n>50, central bars of the notched box represent the median, notches indicate 95% confidential interval, *, p<0.05, One-way ANOVA). (f) growth phenotype and (g) survival rate of *brm5* and *clf29* mutants challenged by 24 hours submergence and recovered for another week (n=3, mean±s.d., *, p<0.05, One-way ANOVA).

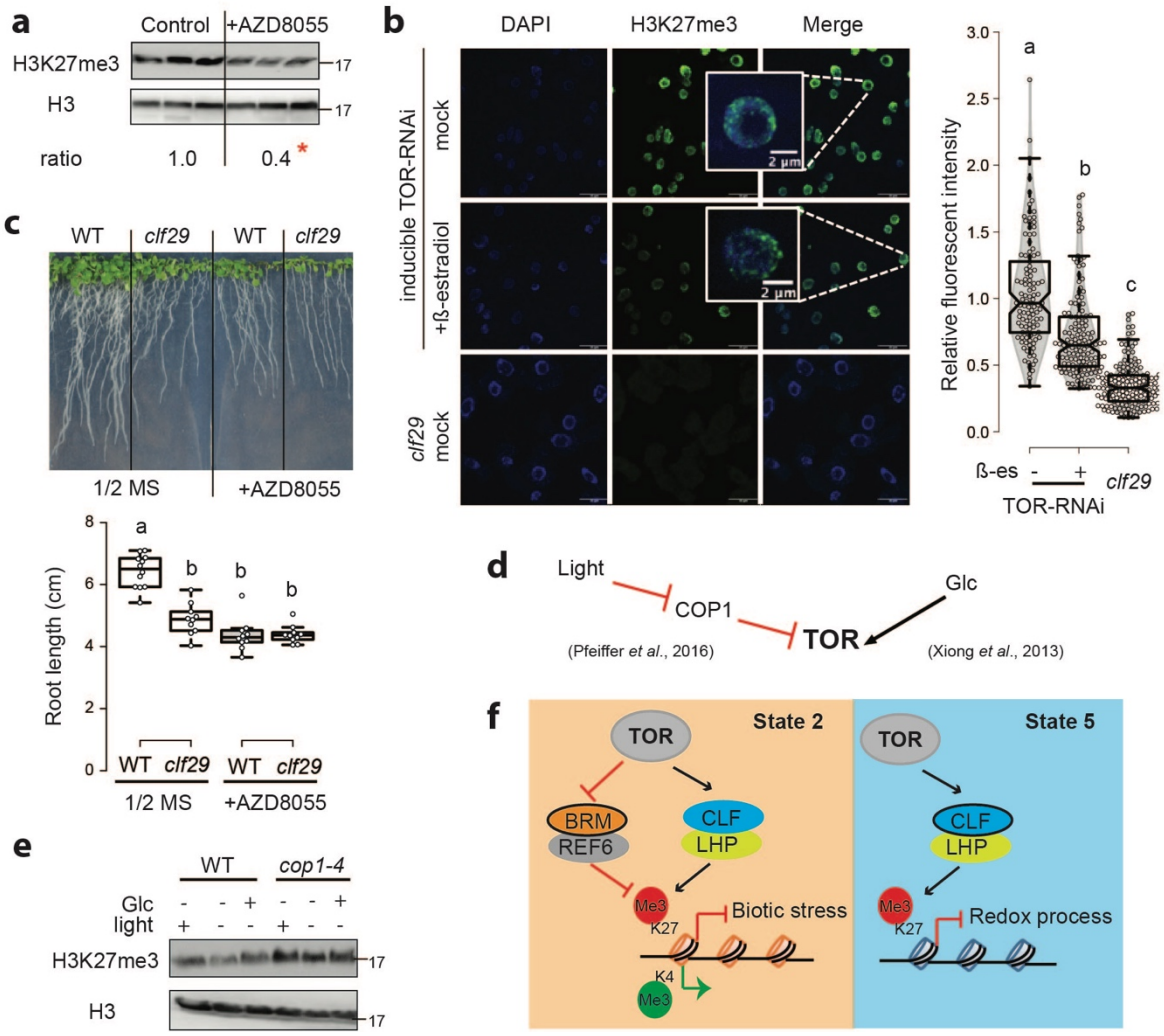

Figure 4 TOR coordinates global H3K27me^3 level at different growth and developmental stages. (a) H3K27me3 level was determined in Arabidopsis leaves treated with 1 µM AZD8055 for 24 hours (n=3, t-test, *, p<0.05). (b) Immuno-staining of H3K27me3 in ß-estradiol inducible TOR-RNAi line and *clf29* mutant. Relative fluorescent signal was normalized against DAPI signal (notches indicate 95% confidential interval, letters indicating statistic difference, One-Way ANOVA, p<0.05). (c) WT and *clf29* were germinated and grown on ½ MS medium or ½ MS supplemented with 0.2 µM AZD for 10 days. Bar, 1.5 cm. Root length was determined (n>10, one-way ANOVA, different letters indicated significant difference, p<0.05). (d) schematic presentation of TOR regulated by light/COP1 or Glucose (Glc) signal. (e) WT and *cop1* mutant were grown under different conditions for 4 days. H3K27me3 and H3 level were determined by western blot. (f) Proposed model of TOR function in controlling genes involved in biotic stress and genes that alter the redox state. We propose the following scenario: active TOR up-regulates CLF and LHP1 to deposit the repressive mark H3K27me3 in the bistable chromatin state 2 (CS2) and the Polycomb-associated chromatin state 5 (CS5). TOR inactivation under biotic stress conditions restores the active CS2 state by BRM that removes the repressive epigenetic mark.

Supplementary table 1: Functional category analysis of genes from each chromatin state (CS).

Chromatin State	GO term	# genes	p-value
CS-1	protein folding	208	5.60E-21
	mRNA processing	139	1.90E-19
	response to cadmium ion	233	8.30E-19
	protein transport	225	4.30E-16
	ribosome biogenesis	112	1.60E-15
	RNA splicing	108	6.10E-15
	intracellular protein transport	138	3.40E-13
CS-2	response to chitin	64	2.70E-06
	response to karrikin	62	2.70E-06
	response to salicylic acid	69	1.60E-05
	response to gibberellin	47	3.00E-04
	defense response	205	3.20E-03
	response to jasmonic acid	62	3.70E-03
	ethylene-activated signaling pathway	69	3.70E-03
CS-3	rRNA modification	7	1.00E+00
	glycosyl compound metabolic process	4	1.00E+00
	translational elongation	24	1.00E+00
CS-4	killing of cells of other organism	137	4.60E-83
	defense response to fungus	145	2.30E-59
	translational elongation	107	3.80E-15
CS-5	regulation of transcription, DNA-templated	494	1.20E-16
	transcription, DNA-templated	445	6.20E-16
	cell differentiation	108	1.20E-14
	SCF-dependent proteasomal ubiquitin-dependent protein catabolic process	66	4.30E-13
	oxidation-reduction process	324	6.40E-13
	hydrogen peroxide catabolic process	46	1.30E-11
	pectin catabolic process	45	2.40E-09
CS-6	protein phosphorylation	113	3.10E-15
CS-7	translational elongation	39	8.00E-25
	translation	39	5.60E-18
CS-8	translational elongation	114	1.10E-66
	translation	124	4.30E-54
	killing of cells of other organism	33	7.70E-13
	defense response to fungus	33	1.80E-07
	oxalate metabolic process	9	4.90E-06
	SCF-dependent proteasomal ubiquitin-dependent protein catabolic process	14	4.40E-04
CS-9	proteolysis	10	9.50E-06

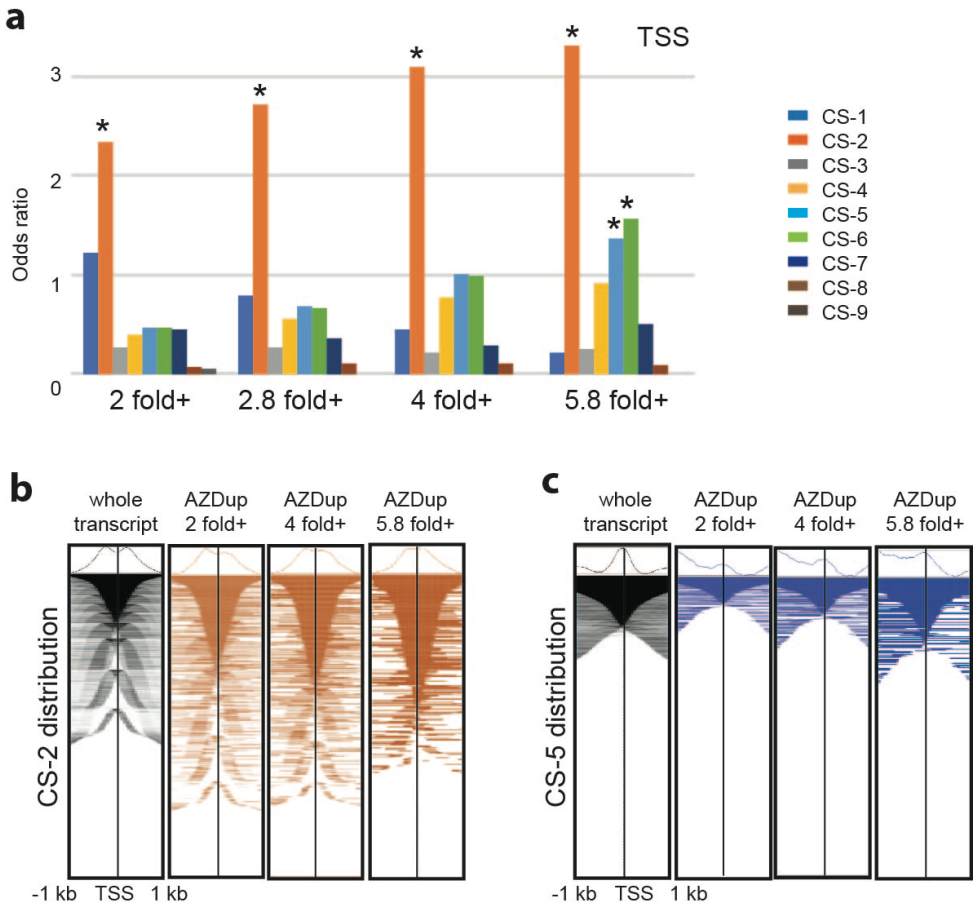

Supplementary figure 1: (a) Enrichment of up-regulated genes by AZD8055 over 2, 2.8, 4 or 5.8 fold at Transcription start site (TSS) (*, OR>1 and p<0.05). (b, c) Heat map presenting the enrichment of up-regulated genes by AZD8055 over 2, 2.8 or 5.8 fold in CS-2 and CS-5 at TSS.

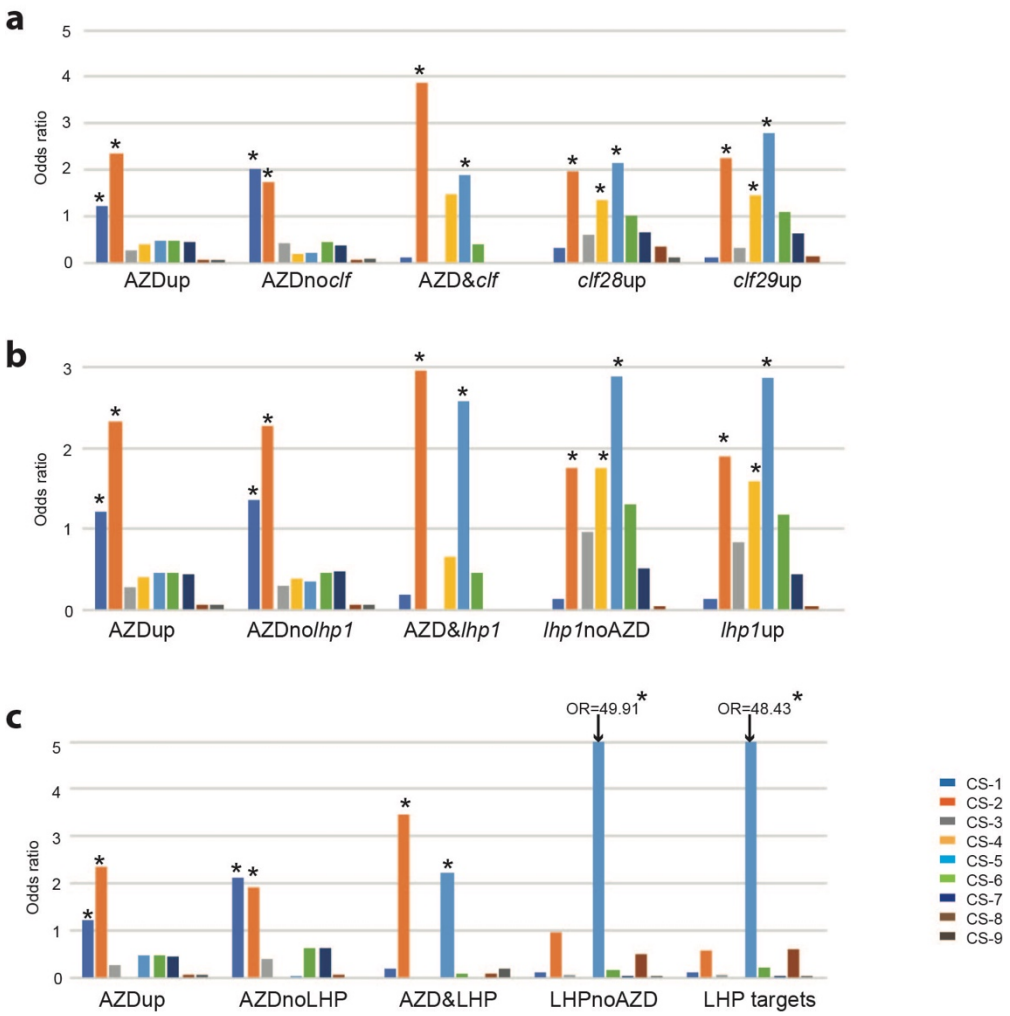

Supplementary figure 2: (a) Enrichment of genes from different intersection between AZDup and up-regulated genes in *clf* mutants presented in fig. 2a. (b) Enrichment of genes from different intersection between AZDup and up-regulated genes in *lhp1* mutants presented in fig. 2e. (c) Enrichment of genes from different intersection between AZDup and LHP1 targets presented in fig. 2g (*, OR>1 and p<0.05).

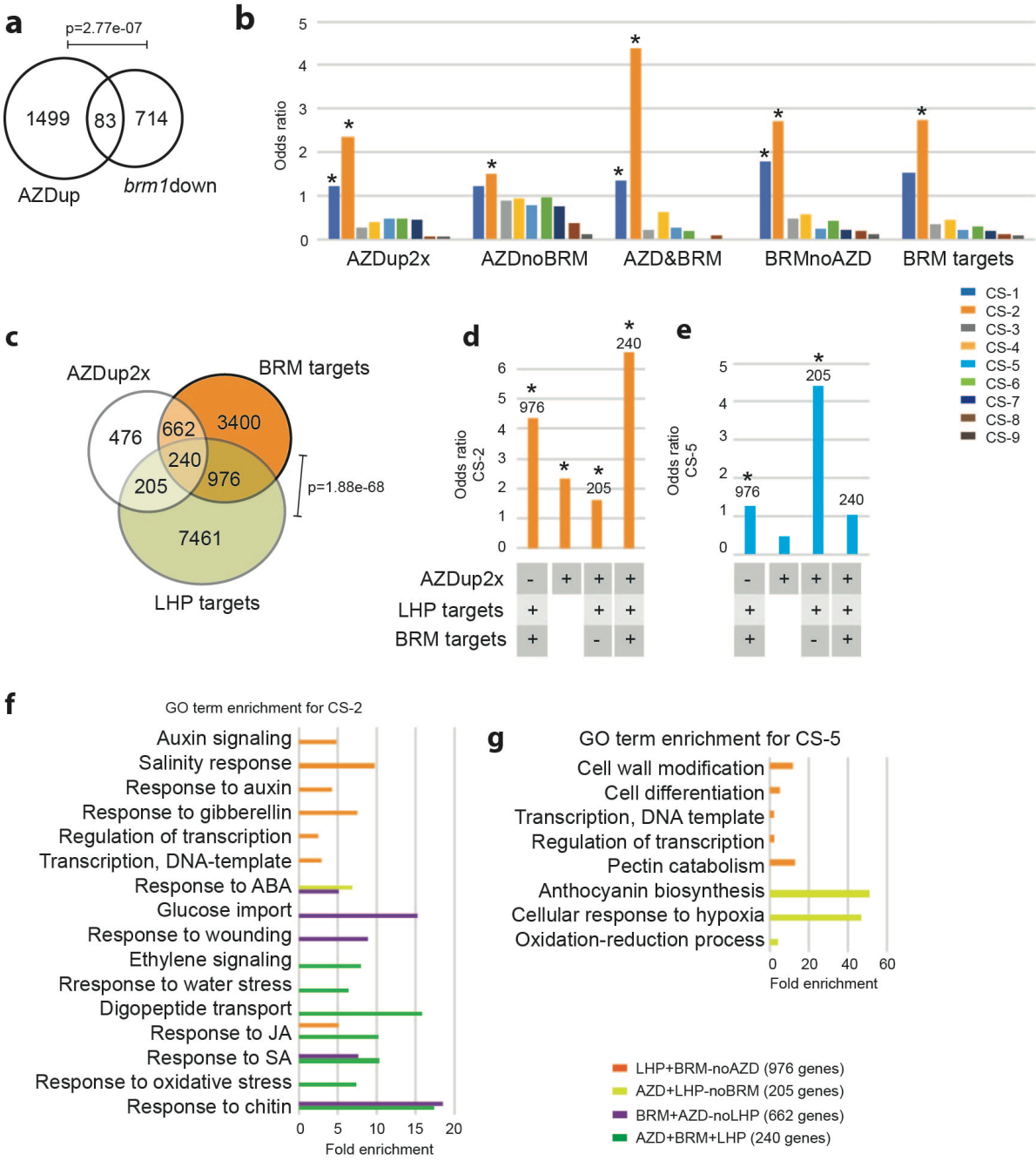

Supplementary figure 3: (a) overlap of up-regulated genes by AZD8055 (AZDup) and down-regulated genes in *brm1* mutant (*brm1*down). P value was calculated by the hypergeometric probability formula (*, p<0.001). (b) CS enrichment of genes from different intersection between AZDup2x and BRM targets presented in fig. 3a (*, OR>1 and p<0.05). (c) overlap of up-regulated genes by AZD8055 (AZDup2x), BRM targets and LHP1 targets (1216 genes, *p<1.88x10^{-68}, hypergeometric test). (d) CS-2 enrichment of genes from different intersections presented in (c) (*, OR>1 and p<0.05). (e) CS-5 enrichment of genes from different intersections presented in (c) (*, OR>1 and p<0.05). (f) Functional category analysis of CS-2 genes from different intersections presented in (c). (g) Functional category analysis of CS-5 genes from different intersections presented in (c). Enrichment was analyzed using total number of genes in the respective state as background (p<0.01, FDR<0.1).

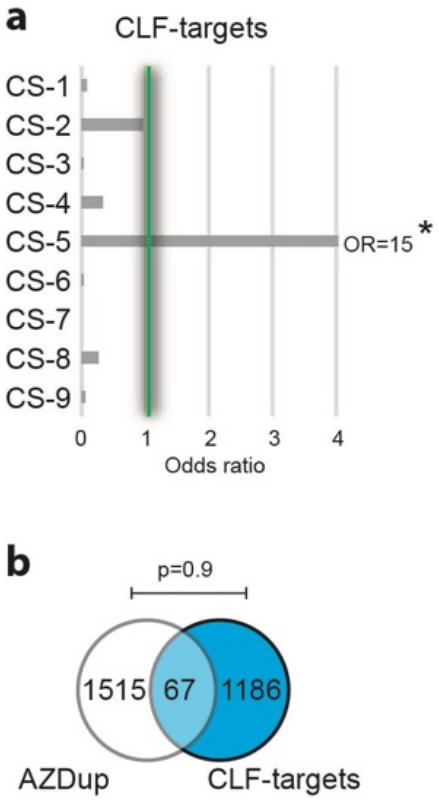

Supplementary figure 4: (a) CS enrichment of CLF targets (*, OR>1 and p<0.05). (b) overlap of up-regulated genes by AZD8055 (AZDup) and CLF targets.